

Enigmatic origin of the largest-known carbon isotope excursion in Earth's history

John P. Grotzinger^{1*}, David A. Fike² and Woodward W. Fischer¹

Carbonate rocks from the Middle Ediacaran period in locations all over the globe record the largest excursion in carbon isotopic compositions in Earth history. This finding suggests a dramatic reorganization of Earth's carbon cycle. Named the Shuram excursion for its original discovery in the Shuram Formation, Oman, the anomaly precedes impressive events in evolution, including the rise of large metazoans and the origin of biomineralization in animals. Instead of a true record of the carbon cycle at the time of sedimentation, the carbon isotope signature recorded in the Shuram excursion could be caused by alteration following deposition of the carbonate sediments, a scenario supported by several geochemical indicators. However, such secondary processes are intrinsically local, which makes it difficult to explain the coincident occurrence of carbon isotope anomalies in numerous records around the globe. Both possibilities are intriguing: if the Shuram excursion preserves a genuine record of ancient seawater chemistry, it reflects a perturbation to the carbon cycle that is stronger than any known perturbations of the modern Earth. If, however, it represents secondary alteration during burial of sediments, then marine sediments must have been globally preconditioned in a unique way, to allow ordinary and local processes to produce an extraordinary and widespread response.

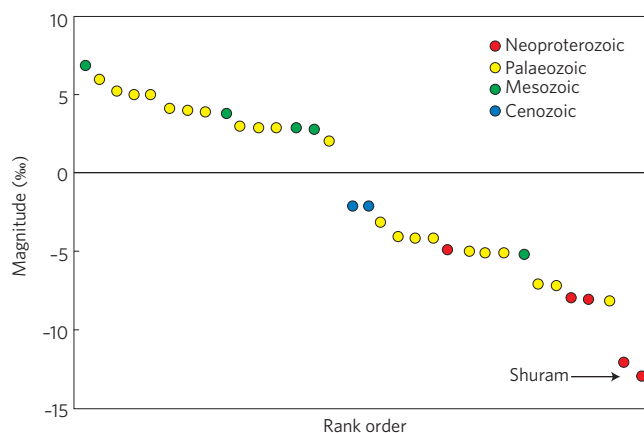
The global carbon cycle is the biogeochemical engine at the heart of acid–base and redox processes in the oceans and atmosphere. It constitutes the most fundamental way in which the biosphere shapes the chemistry of our planet. Studying the behaviour of the carbon cycle during times past, however, presents unique challenges. On geological timescales, the CO₂ emitted from volcanoes and the weathering of sedimentary rocks departs the fluid Earth in two primary sinks — carbonate minerals, and organic carbon; the burial of organic carbon can be linked stoichiometrically to fluxes of O₂ to the atmosphere. Owing to biases intrinsic to the sedimentary record, it is not possible to directly measure the amount of organic carbon buried as a function of time. Instead, geobiologists use carbon isotope ratios in carbonate rocks to constrain the proportional organic carbon burial flux (for example, ref. 1), creating time series data by measuring many samples collected in a stratigraphic section according to height (for example, ref. 2). Ultimately, carbon isotope ratios can provide a measure of the global carbon cycle at the geological instant of sedimentation.

The history of the carbon cycle is recorded in carbonate minerals and organic compounds found in sediments and sedimentary rocks of modern to Archean age^{3–10}. Over the past several decades studies of the chemostratigraphic variation of isotopic carbon have enabled reconstructions of ancient seawater composition including the variation of alkalinity, oxygen, and fluxes of carbon^{2,8,11–15}. The behaviour of the carbon cycle varies over geologic time, marked by different steady states punctuated by brief intervals of anomalous dynamics^{16–22}. These anomalies often signify special events in the history of life, such as the rise of macroscopic and skeletonized animals, as well as mass extinctions^{2,8,16,23–26}.

The secular variability of marine carbon isotope ratios in carbonate-rich sedimentary successions also provides a basis for global correlation¹⁸. Owing to the lack of robust biostratigraphic constraints, construction of 'carbon isotope curves' has seen widespread application to correlate poorly fossiliferous Precambrian strata, particularly those of the Neoproterozoic era¹⁷. Carbon isotopic data typically are

plotted as a function of stratigraphic position^{12,24,27–31} to highlight secular changes in seawater chemistry through time.

As the evaluation of Neoproterozoic chemostratigraphy developed, an extraordinary excursion was discovered in the Ediacaran Shuram Formation, Oman²⁸. Now known as the 'Shuram excursion' (SE), it constitutes one of the most impressive carbon isotopic excursions in Earth history^{32,33}. Plotting, by rank order, the sign and magnitude of carbon isotope excursions recorded over the past 1,000 million years (Myr) shows that the largest anomalies are negative in sign and found in Neoproterozoic strata (Fig. 1). The SE is



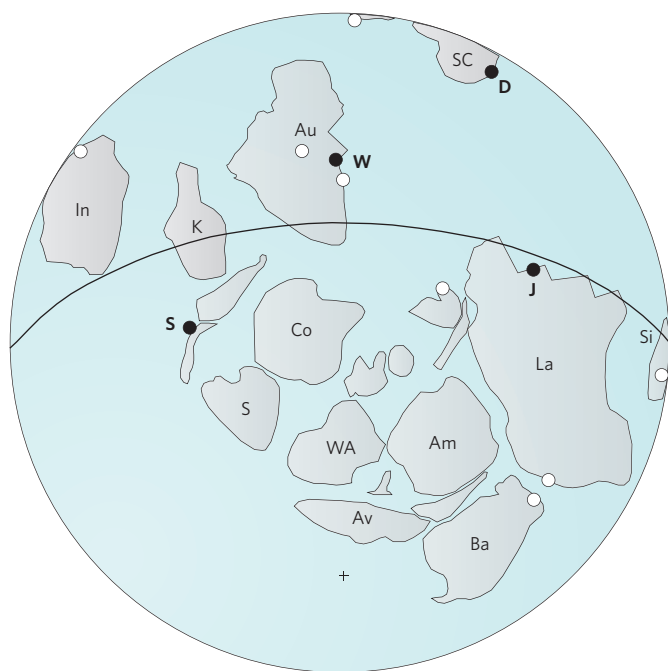


Figure 2 | Palaeogeographic map (600 Myr ago) showing global distribution of the SE. Key sections for the SE are indicated by filled circles (S, Shuram; W, Wonoka; D, Doushantuo; J, Johnnie), and the position of other potential sections that may correlate with the SE are shown as open circles. Am, Amazonia; Au, Australia; Av, Avalonia; Ba, Baltica; Co, Congo; I, India; K, Kalahari; La, Laurentia; S, Sahara; Si, Siberia; SC, South China; WA, Western Australia. Data from ref. 95.

the largest of these, characterized by carbon isotopic values as light as -12‰ (considerably lighter than the input and output fluxes commonly used to constrain isotope mass balance¹), with values less than -6‰ persistent across hundreds of metres of stratigraphic thickness and representing a duration of probably greater than 5 Myr^{28,32–34}. Negative excursions of similar magnitude have been discovered in several other basins including the western United States^{35–37}, South China^{38–40}, South Australia⁴¹, suggesting a primary global event. If primary, the SE would be special for several reasons: first, its magnitude and apparent duration require explanations that differ substantially from the behaviour of the modern carbon cycle (for example, ref. 9); second, the SE has elicited broad use as an Ediacaran chronostratigraphic marker^{17,32,33,37,42–44}; third, several hypotheses link the SE to a putative stepwise increase in the redox potential of ocean basins that influenced the early evolution of macroscopic animals and algae^{2,40,45,46}.

To elaborate on this latter point, the results from models of carbon cycle dynamics suggest that extreme carbon isotope excursions could occur under the conditions of strongly differentiated ocean reservoirs⁹; the SE may have been caused by oxidation of a deep-ocean reservoir charged with dissolved organic carbon^{2,13} (DOC). The demise of this oxygen-limited ocean may have stimulated development of macroscopic metazoans² because oxygen availability has long been regarded as a key factor in the Cambrian radiation of animals¹⁶.

The interpretation of the SE as a record of primary seawater composition has, however, been challenged. Owing to its great magnitude the SE was initially evaluated with appropriate caution and diagenetic alteration was invoked²⁸. (Diagenesis includes those post-depositional processes that involve fluid–rock interaction, such as lithification, recrystallization and loss of primary porosity.) Diagenetic amplification of initially ^{13}C -depleted values also was advocated in subsequent re-evaluation of the SE⁴⁷. This was followed by a wave of

interpretation favouring a primary origin of the SE associated with explanations centred on modes of carbon cycling that are uncharacteristic of the modern Earth^{2,32,33,38,40}. Most recently, the hypothesis that diagenesis could explain the SE has resurfaced^{48,49}.

Despite its potential significance, the genesis of the SE remains unresolved. It is not yet clear whether this extraordinary signal represents a milestone in Earth's environmental evolution, or merely the local expression of carbon recycling during the conversion of sediment to rock. What is clear, however, is the growing set of observations that must be accounted for in any interpretation, including its magnitude, which is unrivalled in the subsequent record of Earth history, and its unique occurrence at this geologic time.

Geologic context of the Shuram excursion

The key observations that must be accounted for in any explanation of the SE include: (1) magnitude, which typically ranges down to -12‰ from previous values as high as $+6\text{‰}$; (2) stratigraphic asymmetry, marked by a rapid drop in $\delta^{13}\text{C}_{\text{carb}}$ values followed by a more gradual recovery; (3) small point-to-point differences between isotope ratios of successive stratigraphic samples; (4) stratigraphic position, sandwiched between Marinoan glacial deposits and Ediacaran macrofossils; (5) inferred long duration represented by hundreds of metres of shallow marine strata; (6) the general lack of time series covariation of carbonate carbon ($\delta^{13}\text{C}_{\text{carb}}$) and organic carbon ($\delta^{13}\text{C}_{\text{org}}$); and (7) a strong correlation between $\delta^{18}\text{O}_{\text{carb}}$ and $\delta^{13}\text{C}_{\text{carb}}$ in many sections.

The SE is best represented by four key stratigraphic sections including the Nafun Group of Oman^{2,28,32,33}, the Wonoka Formation of South Australia⁴¹, the Doushantuo Formation of South China^{39,40} and the Johnnie Formation of the Death Valley region, California^{35–37}; these sections offer independent relative chronologic constraints that alleviate the circularity imposed by using the SE itself to establish correlations. The SE is constrained in age to postdate strata containing Marinoan glacial deposits, including cap carbonates (~ 630 Myr ago), and predate Ediacaran macrofossil-bearing strata and/or the Precambrian/Cambrian boundary (542 Myr ago). In South Australia and Death Valley, strata containing the SE are overlain by strata containing Ediacaran soft-bodied macrofossils^{35,41,50}. In Oman, strata that postdate the SE contain skeletal fossils of the *Cloudina* association²⁵.

A large number of additional globally dispersed sections (Fig. 2) have been correlated with the SE (Fig. 3). Although they share a

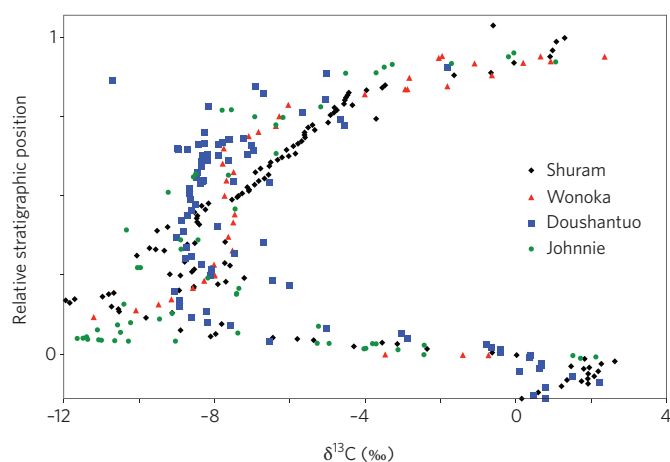


Figure 3 | Magnitude and asymmetry of SE. Data from four key sections (Shuram Formation, Oman²; Wonoka Formation, South Australia⁴¹; Doushantuo Formation, South China⁴⁰; Johnnie Formation, southeast California³⁷) are superimposed and normalized to the thickness of the SE in Oman using $\delta^{13}\text{C}$ zero crossings.

similar chemostratigraphic pattern, they lack sufficient independent constraints to provide a strong relative chronology. For example, Neoproterozoic strata in Scandinavia show strongly negative $\delta^{13}\text{C}_{\text{carb}}$ values over a substantial thickness⁴³, however, the section is structurally complicated and lacks definitive fossils, so its inferred Ediacaran age is not secure. Other globally distributed carbonate-bearing Ediacaran strata (for example, India, Scotland, Siberia and Uruguay^{44,51–53}) contain evidence for significant negative isotopic excursions, but none are as negative or as thick as the SE. Therefore, global correlation of the SE is supported by at least four, and possibly as many as nine, stratigraphic sections (Fig. 2).

An important attribute of the four key sections is the significant stratigraphic thickness of the SE. In Oman, this spans ~400 m (ref. 32,33), in Death Valley 300–500 m (ref. 37) and in South Australia ~150 m (ref. 41). The Doushantuo SE is considerably thinner (50 m) relative to the other key sections, probably owing to condensation of the section. Simple calculations based on inferences of basin subsidence rate^{32,33} and interpolation between geochronologic tie points³⁴ yield estimates for the duration of the SE of 5–50 Myr. The important point is that even the shortest estimate is almost an order of magnitude greater than the expected residence time of carbon in the ocean and atmosphere, pointing to a potentially non-uniformitarian process of formation for the SE.

In the four key sections the SE shows a rapid drop to the most negative $\delta^{13}\text{C}_{\text{carb}}$ values, followed by a slow recovery to less negative and eventually positive values (Fig. 3). In Oman, this trend begins in the underlying Khufai Formation carbonates and continues into the mixed carbonate and siliciclastics of the overlying Shuram Formation^{32,33}. The most negative values are achieved in the transgressive system tract of the lower Shuram Formation⁴⁷, suggesting that sedimentary condensation may in part be responsible for the asymmetric expression of the SE. The sections in Australia and Death Valley show similar relationships, with the drop recorded in transgressive to early highstand depositional systems tracts^{35,41,54,55}. These observations suggest that the stratigraphic shape of the SE is related to transgressive condensation of strata that embrace the decline to the most negative values. In contrast, the SE in the Doushantuo is interpreted as a highstand, rather than transgressive, deposit⁴⁰ and therefore shows a more symmetrical shape (Fig. 3).

The SE is recorded in a variety of facies associations that define storm-dominated, prograding shelf environments composed of open marine sediments^{32,33,54,55}. Carbonates analysed for carbon isotopic values typically include coarse-grained facies such as trough cross-bedded ooid grainstones, hummocky cross-stratified intraclast–ooid grainstones, and flat-pebble conglomerates (Fig. 4). Finer-grained facies are also present and consist of silt to fine-sand-sized carbonate sediments with wave-ripple cross-stratification and small-scale hummocky cross-stratification. Mud-sized carbonates form discrete interbeds in fine-grained shales and quartz siltstones. Where the flux of fine-grained siliciclastic sediments was high, carbonate mudstones may be preserved only as concretions, but this is the exception rather than the rule.

Finally, the four key stratigraphic sections of the SE are located in significantly different palaeogeographic locations, as are the other supporting sections (Fig. 2). This requires the SE to be global in extent.

The case for primary signal

By convention, carbon isotope ratio data are interpreted in the context of isotope mass balance, with an input value of approximately -6‰ (mantle values⁵⁶) to the global ocean. If primary, the constraint imposed by the SE is for the isotopic composition of the carbon entering the oceanic reservoir of dissolved inorganic carbon (DIC) to be characterized by very low values ($\leq -12\text{‰}$). Inputs this low presumably reflect a source of CO_2 derived from the oxidation of a reservoir of organic carbon (which is characterized by

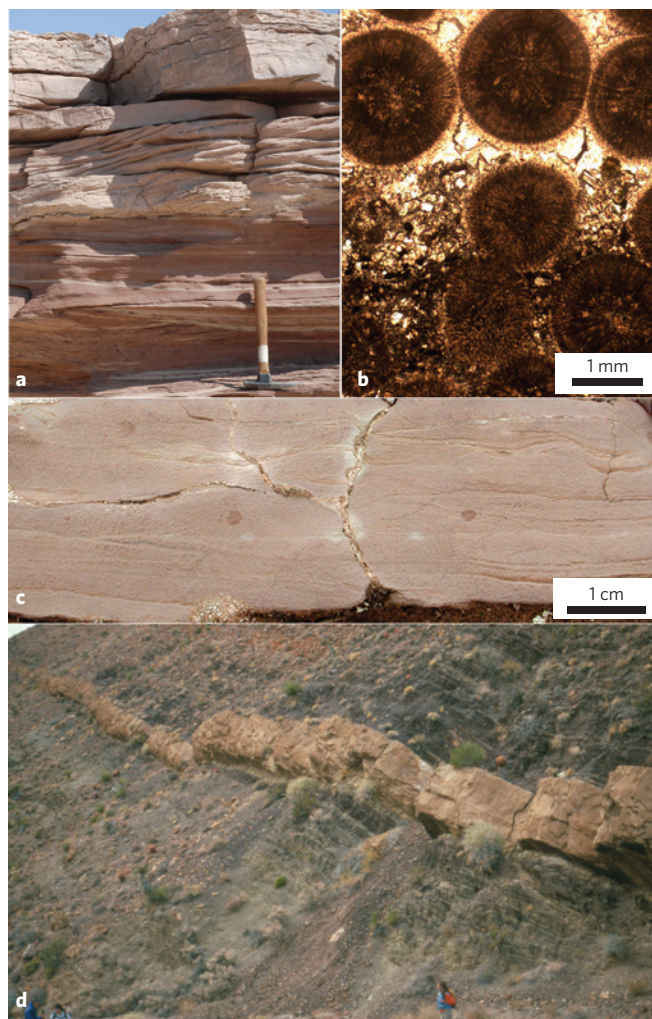


Figure 4 | Representative depositional facies from strata that preserve the SE. **a**, Hummocky cross-stratified intraclast–ooid grainstone (limestone) in Shuram Formation, Oman. **b**, Ooid grainstone/packstone (limestone) in Shuram Formation, Oman. **c**, Wave-ripple cross-stratified peloidal grainstone (limestone), Wonoka Formation, Australia. **d**, Trough cross-bedded ooid grainstone (dolostone) interbedded with organic-lean red shales in Johnnie Formation, California.

$\delta^{13}\text{C}$ values of -25‰ to -35‰), be it ancient sedimentary carbon or carbon from within the ocean itself. Support for oxidation of a pre-existing reduced reservoir at the onset of the SE is also provided by sulphur isotope data^{2,36,40}. Carbonate-associated sulphate reveals a systematic decrease in $\delta^{34}\text{S}$ whereas a parallel decrease in $\delta^{34}\text{S}$ occurs in coeval pyrite^{2,36,40}.

The observed pattern of systematically variable $\delta^{13}\text{C}_{\text{carb}}$ data and relatively invariant $\delta^{13}\text{C}_{\text{org}}$ data^{2,40,41} was explored using a new model of the carbon cycle⁹. This model invoked a large dissolved and/or finely particulate organic carbon reservoir in the ocean, one that was substantially larger — and characterized by a longer residence time — than the coeval DIC pool. In this framework, oxidation of a portion of the ^{13}C -depleted DOC reservoir to CO_2 would have resulted in a corresponding isotopic depletion of the DIC reservoir, which was recorded in coeval marine carbonates. For $\delta^{13}\text{C}_{\text{org}}$ to remain essentially invariant in this scenario, it must be overwhelmingly sourced from ‘fossil carbon’ of the DOC reservoir directly and not from DIC-derived primary productivity. This hypothesis describes a carbon cycle that is very different from organic carbon delivery to sediments today.

The idea of a large DOC reservoir of Ediacaran age has garnered support^{2,36,40}, but see ref. 57 for a contrary hypothesis. Wide acceptance will require resolution of several inconsistencies. For example, a large DOC reservoir predicts uniform $\delta^{13}\text{C}_{\text{org}}$ values for globally distributed strata; but $\delta^{13}\text{C}_{\text{org}}$ values vary between different SE sections^{2,40,41}. This variability, however, may reflect non-uniform and often low concentrations of organic matter². Indeed, a sharp enrichment in $\delta^{13}\text{C}_{\text{org}}$ at the base of the SE corresponds to a decrease in total organic carbon content²; this trend is common in the geologic record⁵⁸ and may result from post-depositional loss of organics (for example, diagenetic remineralization or thermal cracking) or analytical challenges with measuring rocks of low organic carbon content. Perhaps the largest challenge concerns the chemical and physical nature of the DOC pool and the oxidant budget required to oxidize it to DIC. Simple calculations suggest that the required flux of oxidants would be equal to that available at the surface of the Earth today⁵⁹. Furthermore, if the source of oxidants was largely O_2 in the atmosphere, it is unclear what processes kept these oxidants and DOC separate for long periods of time (> 1 Myr), only to reintroduce them at the onset of the SE. These discordances highlight the need for development of further hypotheses and measurements that seek to uncover the processes responsible for the pattern of the SE. Most recently, a new hypothesis that emphasizes the primary nature of the SE has been proposed⁶⁰. This work involves considerations of the importance of methane cycling.

The case for diagenesis

Carbonate rocks commonly recrystallize and re-equilibrate with pore fluids during diagenesis, complicating the interpretation of chemostratigraphic data. Large $\delta^{18}\text{O}_{\text{carb}}$ depletion relative to sea water is considered a hallmark of diagenesis, marked by resetting of primary oxygen isotope ratios^{61–64}. Consequently, many early studies of Neoproterozoic carbonates employed established techniques developed for the screening of diagenetic processes, such as the retention or loss of mobile trace elements (for example, Sr, Fe and Mn), $^{18}\text{O}/^{16}\text{O}$ ratios and $^{87}\text{Sr}/^{86}\text{Sr}$ ratios^{27,28,31,65–67}. Because oxygen is a principal element of water and carbon is a minor constituent it was proposed that alteration of carbon and oxygen isotope ratios in carbonate rocks should follow a curve with water-to-rock ratios described by a model of two components mixing⁶³. This framework suggests that carbon isotope ratios should be differentially buffered against post-depositional changes in composition. Nonetheless, because the strongly negative $\delta^{13}\text{C}_{\text{carb}}$ values (-12‰) of the SE fell outside the standard operation of the carbon cycle⁵⁶, early researchers^{28,47} attributed the SE in part to diagenetic alteration.

Geochemical data support the inference of diagenesis in many sections recording the SE, in particular, the covariation of $\delta^{13}\text{C}_{\text{carb}}$ and $\delta^{18}\text{O}_{\text{carb}}$ (Fig. 5)^{2,41}. We know empirically that there is often a covariation between these measurements in suites of samples that have undergone extensive diagenesis. Furthermore, because the SE is poorly recorded in the carbon isotope ratios of organic phases in the same rocks (manifest as a lack of covariation in $\delta^{13}\text{C}_{\text{org}}$ and $\delta^{13}\text{C}_{\text{carb}}$)^{2,40,41} (Fig. 5), this supports the hypothesis that the SE chemostratigraphic pattern is solely the result of diagenetic processes^{48,49}.

In one hypothesis, reaction of SE sediments with ^{13}C -depleted meteoric waters is inferred to have generated the SE pattern^{28,47,48}. Meteoric waters are characterized by negative $\delta^{18}\text{O}$ values and can acquire ^{13}C -depleted DIC from the oxidation of terrestrial organic carbon⁶⁸. Diagenetic alteration of carbonates from meteoric fluids can produce ^{13}C -depleted isotope ratios and co-variation with $\delta^{18}\text{O}$ values. This pattern is clearly recorded in Miocene–Recent platform sediments in the Bahamas, where this alteration was facilitated in large part by high amplitude sea-level changes tied to glaciation⁶⁹. The isotopic pattern produced by this process is similar in sign to the SE, but not in magnitude. Furthermore, the Bahamian rocks show evidence of many episodes of subaerial exposure⁷⁰. Exposure

processes are also recorded by increased stratigraphic variability in point-to-point differences between successive stratigraphic samples⁷⁰. Neither of these aspects are observed in SE strata. Moreover, the hypothesis that the SE pattern is a result of meteoric diagenesis carries an interesting corollary, because it requires the influence of a conspicuous reservoir of terrestrial organic carbon. Therefore, in one instance⁴⁸ the Neoproterozoic landscape is predicted to be as productive as younger Phanerozoic landscapes, despite the dearth of supporting palaeontological evidence. Nevertheless, assuming this hypothesis is correct, one would expect extreme excursions such as the SE to become progressively more common after the evolution and rise of vascular land plants — which definitively increased the terrestrial biomass relative to earlier times^{71–73}. However, isotopic excursions of the same magnitude or duration (in rock space) as the SE are unknown in Phanerozoic strata^{18,19} (Fig. 1).

Another mechanism potentially responsible for diagenetic alteration of carbon isotope ratios results from fluid–rock interactions driven by advection of hydrocarbon-influenced basinal fluids during burial and sediment compaction. This process involves oxidation of previously deposited organic matter to form a source of ^{13}C -depleted carbonate cements and replacement textures. In some SE sections, the co-variation of carbon and oxygen coupled with the occurrence of organic-rich shales supports the hypothesis that burial diagenesis could have produced extremely depleted carbonates⁴⁹. Whereas some of the key sections contain organic-rich shales (Duoshantuo, locally the Shuram), others do not (Wonoka, Johnnie, generally the Shuram). Furthermore, in the case of both the Shuram and Doushantuo Formations, the $\delta^{13}\text{C}_{\text{carb}}$ profiles show increased point-to-point variability in the organic-rich parts of the sections. For example, the organic-rich carbonate rocks below the EN2 excursion of the Duoshantuo Formation show larger variance than those in the EN3 excursion⁴⁰. This pattern suggests local alteration of the rocks in the vicinity of the organic-rich facies. However, in the organic-lean facies that compose the EN3 excursion — interpreted as the equivalent of the SE — the ^{13}C -depletion is far greater than in the EN2, but yet the data show a striking point-to-point coherence.

The small first differences in $\delta^{13}\text{C}_{\text{carb}}$ between samples aligned with stratigraphic height are an important attribute observed in the key sections. For example, small point-to-point variations are observed for data from Nafun Group (Oman), despite significant point-to-point changes in sedimentary facies. This diversity of facies had different initial porosities and permeabilities (consider an ooid grainstone versus lime mudstone), and therefore different reactivities regarding diagenetic fluid flow and water–rock interaction. A paradox thus emerges in which the rocks that are proposed to be the most altered show the least spread in the $\delta^{13}\text{C}_{\text{carb}}$ values as a function of stratigraphic position. At face value, this is not consistent with diagenetic alteration of a rock whose starting composition is proposed to be 0‰. One would expect to see a much greater degree of scatter in the stratigraphic expression of severely ^{13}C -depleted carbon isotope ratios if they arose from burial diagenesis.

It is noteworthy that there are no known isotopic excursions of either the magnitude or thickness of the SE in Phanerozoic geologic history (Fig. 1)^{18,19}. Yet in this same interval of time we see preserved all of the world's great globally distributed petroleum source rocks⁷⁴. Many are in direct contact with carbonates, or even form the down-dip facies of self-sourcing reservoirs, such as the Jurassic Smackover Formation. The Smackover has been intensely studied to understand its diagenesis and in some cases was subjected to significant burial depths and temperatures⁷⁵, at least as great as what is observed for the Shuram Formation^{76–78}. Despite the compelling case to be made for burial diagenesis⁷⁹, petroleum migration and even *in situ* oxidation of organic matter⁸⁰, no section of Smackover stratigraphy has been identified that shows depletion similar to what is known from the SE. The same is true for the Ediacaran Khatyspyt Formation in Siberia, a known source rock and petroliferous limestone⁸¹. Despite

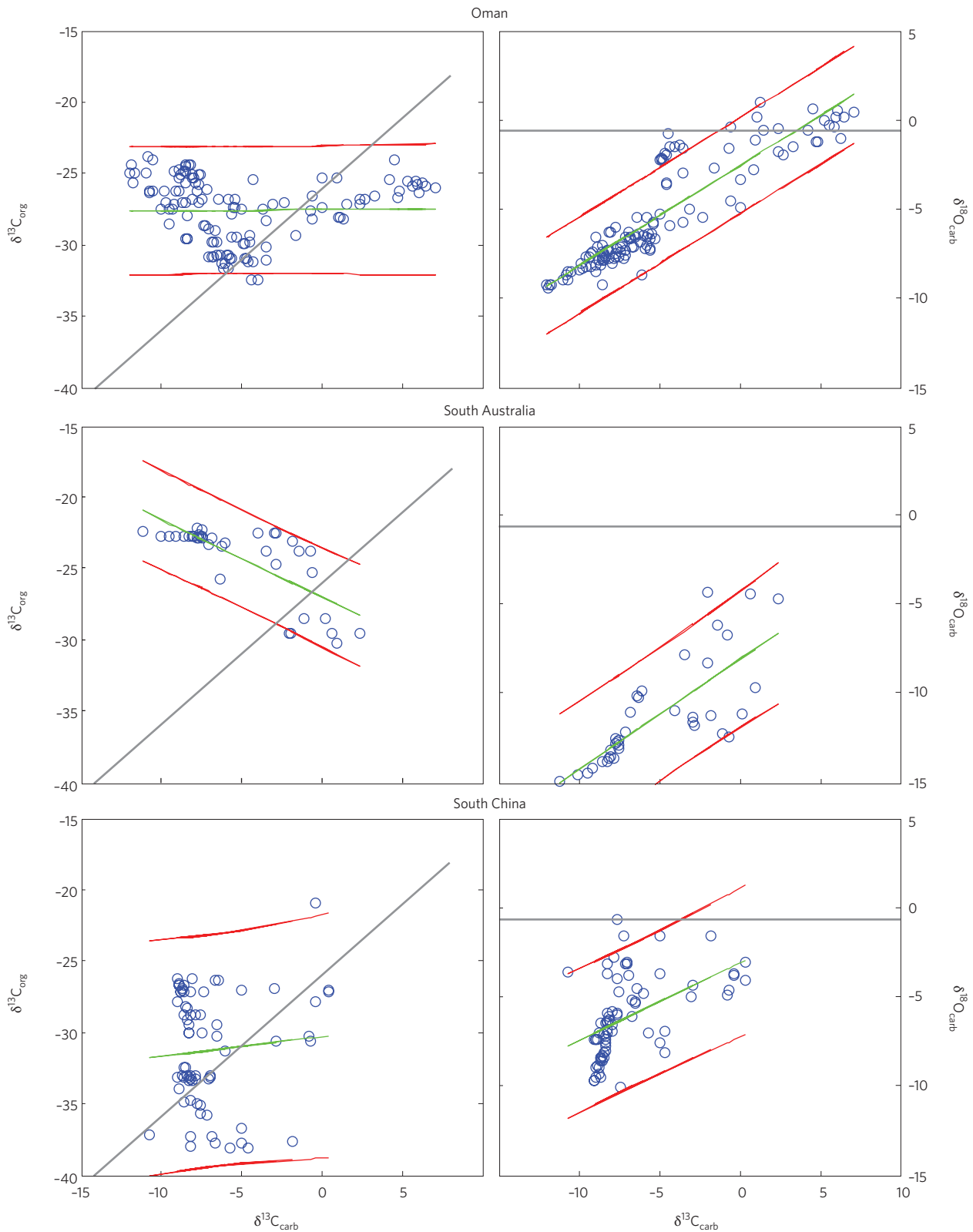


Figure 5 | Geochemical cross plots of SE sections. Paired isotopic data are shown from Oman, South China and South Australia. Left panels, $\delta^{13}\text{C}_{\text{carb}}$ versus $\delta^{13}\text{C}_{\text{org}}$. Right panels, $\delta^{13}\text{C}_{\text{carb}}$ versus $\delta^{18}\text{O}_{\text{carb}}$. Also shown are relationships estimated by OLS regressions with 95% confidence intervals. Based on an understanding of the Earth's modern carbon cycle and assuming no diagenesis, if the SE records a primary signal based on changing organic carbon burial or $\delta^{13}\text{C}$ delivery to the ocean, then the left panels should show a correlation with an expected slope of 1, and the right panels should show no correlation with an expected slope of 0. Each of these panels shows data relationships that are statistically discordant with these predictions. The lowermost left panel (South China $\delta^{13}\text{C}_{\text{carb}}$ versus $\delta^{13}\text{C}_{\text{org}}$) is the only section that shows a significant negative slope and confidence intervals that overlap with the predictions. Note the strong correlation between $\delta^{13}\text{C}$ and $\delta^{18}\text{O}$ in all three locations, a classic indicator of diagenetic water-rock interaction. Data taken from refs 2, 40 and 41.

high-resolution chemostratigraphic studies^{82–84} this organic-rich unit displays uniform values of +1 to +2‰. Therefore, it seems that ordinary burial diagenesis also cannot account for the unique attributes of the SE. Though it is clear that many SE sections show the hallmark patterns of post-depositional alteration, if the unique carbon isotope pattern is attributed to diagenetic processes, it must have resulted from a style of diagenesis not observed in younger strata.

Extraordinary processes of Ediacaran age

The SE presents a biogeochemical enigma. Its stratigraphic context provides substantial evidence for a global palaeoceanographic event; however, this interpretation is seemingly contradicted by the lack of covarying $\delta^{13}\text{C}_{\text{carb}}-\delta^{13}\text{C}_{\text{org}}$ data and by the strong correlation between carbonate carbon and oxygen isotope ratios, a hallmark of open-system diagenesis in sedimentary basins. Were it not for its extreme magnitude, displayed over such a substantial thickness of rock and in globally distributed localities, the SE could be simply dismissed as a result of local diagenesis. The record of diagenesis observed in the most recent 500 Myr of Earth history provides evidence for only modest alteration of primary signals. Curiously, to find something as large as the SE one must go back further in time, not forward⁸⁴. In this regard, the SE chemostratigraphic pattern is not well explained by hypotheses that invoke business-as-usual diagenetic mechanisms. All proposed mechanisms for diagenesis fall short in attempting to account for the magnitude of the SE without also explaining the absence of such large signals in the Phanerozoic record.

Yet geology is about what happened — not what should have happened. What can be stated unequivocally is that in at least four globally distributed localities there is a single event of Ediacaran age that involves extreme ^{13}C depletion over circa 100-m-scale stratigraphic thicknesses of carbonate rock. This observation, strengthened by the past decade of work, must be held at the core of any phenomenological explanation of the SE. The importance of stratigraphic context has enabled evaluation of other great geologic controversies whose explanation involves unexpected and often extraordinary processes (for example, Messinian salinity crisis⁸⁵; Cretaceous/Tertiary extinction^{86,87}; Permian/Triassic extinction^{88,89}; and Neoproterozoic Snowball Earth⁹⁰). Similarly, it is prudent to honour stratigraphic context in evaluating possible origins of the SE.

The balance of evidence at this point suggests the possibility of an exotic mechanism: a global diagenetic event. The most obvious scenario would involve global sea-level fall associated with the onset of glacial conditions^{91,92}. This hypothesis was suggested during presentations at the 2010 meeting of the Geological Society of America. Very simply, the concept involves globally synchronous oscillations of sea level that drive fluid flow in sedimentary basins to produce globally synchronous but locally expressed diagenetic overprints (L. Derry and P. Swart, personal communication). Although the possibility that significant ice existed during SE time cannot be excluded³⁴, it has been shown that the well-known Gaskiers glacial event is likely to pre-date the SE⁴⁴. Furthermore, three additional observations cannot be accounted for by a global sea-level fall: SE strata comprised of transgressive to highstand facies; the lack of karst or other subaerial exposure surfaces superjacent to the SE; and the absence of isotope excursions of a similar magnitude associated with strata deposited during periods of known sea-level drawdown^{18,32,33,37,40,41}. Finally, we note that for well-documented Proterozoic exposure surfaces, which provide definitive evidence in the form of karst for invasion of and reaction with meteoric fluids, there is no evidence for carbon isotope ratios below -2 to -5 ‰^{93,94}. Therefore, we consider a different mechanism by which sediments were deposited under temporally focused and globally pervasive conditions that affected their primary composition, so that the sediments were preconditioned to subsequently influence their reaction potential during burial and diagenesis.

One scenario would propose that the primary inorganic composition of sediments was affected by a significant perturbation in global redox, driven by a rise in atmospheric oxygen. This could have created a set of conditions wherein sediments were primed to more efficiently oxidize organic compounds that they encounter, either delivered by sinking particles through the water column, or later through diagenesis driven by migrating hydrocarbon-rich fluids, thereby producing greater amounts of ^{13}C -depleted DIC with the potential for ubiquitous alteration of carbonate rocks. The primer would necessarily be sediment composition, enriched in mineral electron acceptors (for example, ferric hydroxides, sulphates) with high oxidizing potential. The essential point is that such a process would tie to a unique interval in Earth history, of global extent, that also accounts for the evidence for local diagenesis. This hypothesis explains several of the unique attributes of the SE; however, no appropriate data exist to test it. Although we lack confidence at this time in this (and other) potential scenarios for global diagenesis, we suggest that consideration of such extraordinary mechanisms could be a good starting point to construct a hypothesis that honours all of the observations and data.

The Ediacaran enigma

For the time being, the SE must be viewed from several perspectives. If it reflects primary seawater composition and perturbation of marine DIC, then we must explain the strong correlation between carbon and oxygen isotopic values that cannot be accounted for in present carbon cycle models. If the SE is diagenetic in origin, then perhaps we need to search for an explanation that can account for its apparently global distribution — a mechanism that would predict enhanced chemical modification of buried sediments of very similar or possibly identical age. From either perspective, the SE presents a tough problem, and one that is ripe for fresh approaches and ideas.

References

- Kump, L. R. & Arthur, M. A. Interpreting carbon-isotope excursions: carbonates and organic matter. *Chem. Geol.* **161**, 181–198 (1999).
- Fike, D. A., Grotzinger, J. P., Pratt, L. M. & Summons, R. E. Oxidation of the Ediacaran Ocean. *Nature* **444**, 744–747 (2006).
- Holland, H. D. *The Chemical Evolution of the Atmosphere and Oceans* (Princeton Univ. Press, 1984).
- Schidlowski, M. A 3,800-million-year isotopic record of life from carbon in sedimentary rocks. *Nature* **333**, 313–318 (1988).
- Holser, W. T., Schidlowski, M., Mackenzie, F. T. & Maynard, J. B. in *Chemical Cycles in the Evolution of the Earth* (eds Gregor, C. B., Garrels, R. M., Mackenzie, F. T. & Maynard, J. B.) 105–173 (Wiley, 1988).
- Des Marais, D. J. *et al.* in *The Proterozoic Biosphere: A Multidisciplinary Study* (eds Schopf, W. J. & Klein, C.) 325–334 (Cambridge Univ. Press, 1992).
- Hayes, J. M., Strauss, H. & Kaufman, A. J. The abundance of C-13 in marine organic matter and isotopic fractionation in the global biogeochemical cycle of carbon during the past 800 Ma. *Chem. Geol.* **161**, 103–125 (1999).
- Hoffman, P. F., Kaufman, A. J., Halverson, G. P. & Schrag, D. P. A Neoproterozoic Snowball Earth. *Science* **281**, 1342–1346 (1998).
- Rothman, D. H., Hayes, J. M. & Summons, R. E. Dynamics of the Neoproterozoic carbon cycle. *Proc. Natl Acad. Sci. USA* **100**, 8124–8129 (2003).
- Sageman, B. B. *et al.* A tale of shales: the relative roles of production, decomposition, and dilution in the accumulation of organic-rich strata, Middle-Upper Devonian, Appalachian basin. *Chem. Geol.* **195**, 229–273 (2003).
- Berner, R. A. & Raiswell, R. Burial of organic carbon and pyrite sulfur in sediments over Phanerozoic time: a new theory. *Geochem. Cosmochim. Acta* **47**, 855–862 (1983).
- Knoll, A. H., Hayes, J. M., Kaufman, A. J., Swett, K. & Lambert, I. B. Secular variation in carbon isotope ratios from Upper Proterozoic successions of Svalbard and East Greenland. *Nature* **321**, 832–838 (1986).
- Fike, D. A. & Grotzinger, J. P. A paired sulfate-pyrite $\delta^{34}\text{S}$ approach to understanding the evolution of the Ediacaran-Cambrian sulfur cycle. *Geochem. Cosmochim. Acta* **72**, 2636–2648 (2008).
- Higgins, J. A., Fischer, W. W. & Schrag, D. P. Oxygenation of the ocean and sediments: consequences for the seafloor carbonate factory. *Earth Planet. Sci. Lett.* **284**, 25–33 (2009).

15. Fischer, W. W. *et al.* Isotopic constraints on the Late Archean carbon cycle from the Transvaal Supergroup along the western margin of the Kaapvaal Craton, South Africa. *Precamb. Res.* **169**, 15–27 (2009).
16. Knoll, A. H. & Carroll, S. B. Early animal evolution: emerging views from comparative biology and geology. *Science* **284**, 2129–2137 (1999).
17. Halverson, G. P., Maloof, A. C. & Hoffman, P. F. Towards a Neoproterozoic composite carbon-isotope record. *Geol. Soc. Am. Bull.* **117**, 1181–1207 (2005).
18. Saltzman, M. R. in *A Geologic Time Scale* (Cambridge Univ. Press, in the press).
19. Shields, G. & Veizer, J. Precambrian marine carbonate isotope database: version 1.1. *Geochem. Geophys. Geosyst.* **3**, 1031 (2002).
20. Payne, J. L. *et al.* Large perturbations of the carbon cycle during recovery from the end-Permian extinction. *Science* **305**, 506–509 (2004).
21. Maloof, A. C., Schrag, D. P., Crowley, J. L. & Bowring, S. A. An expanded record of Early Cambrian carbon cycling from the Anti-Atlas Margin, Morocco. *Can. J. Earth Sci.* **42**, 2195–2216 (2005).
22. Zachos, J. C., Dickens, G. R. & Zeebe, R. E. An early Cenozoic perspective on greenhouse warming and carbon-cycle dynamics. *Nature* **451**, 279–283 (2008).
23. Holser, W. T. Catastrophic chemical events in the history of the ocean. *Nature* **267**, 403–408 (1977).
24. Grotzinger, J. P., Bowring, B. Z., Saylor, B. Z. & Kaufman, A. J. Biostratigraphic and geochronologic constraints on early animal evolution. *Science* **270**, 598–604 (1995).
25. Anthor, J. E. *et al.* Extinction of Cloudina and Namacalathus at the Precambrian-Cambrian boundary in Oman. *Geology* **31**, 431–434 (2003).
26. Maloof, A. C. *et al.* The earliest Cambrian record of animals and ocean geochemical change. *Geol. Soc. Am. Bull.* **122**, 1731–1774 (2010).
27. Pell, S. D., McKirdy, D. M., Jansyn, J. & Jenkins, R. J. F. Ediacaran carbon isotope stratigraphy of South Australia. *Trans. R. Soc. South Aust.* **117**, 153–161 (1993).
28. Burns, S. J. & Matter, A. Carbon isotopic record of the latest Proterozoic from Oman. *Eclogae Geol. Helv.* **86**, 595–607 (1993).
29. Narbonne, G. M., Kaufman, A. J. & Knoll, A. H. Integrated chemostratigraphy and biostratigraphy of the Windermere Supergroup, northwestern Canada: implications for Neoproterozoic correlations and the evolution of animals. *Geol. Soc. Am. Bull.* **106**, 1281–1292 (1994).
30. Brasier, M. D., Shields, G., Kuleshov, V. N. & Zhegallo, E. A. Integrated chemo- and biostratigraphic calibration of early animal evolution: Neoproterozoic-early Cambrian of southwest Mongolia. *Geol. Mag.* **133**, 445–485 (1996).
31. Saylor, B. Z., Kaufman, A. J., Grotzinger, J. P. & Urban, F. A composite reference section for terminal Proterozoic strata of southern Namibia. *J. Sedim. Res.* **66**, 1178–1195 (1998).
32. Le Guerroue, E., Allen, P. A. & Cozzi, A. Chemostratigraphic and sedimentological framework of the largest negative carbon isotopic excursion in Earth history: the Neoproterozoic Shuram Formation (Nafun Group, Oman). *Precamb. Res.* **146**, 68–92 (2006).
33. Le Guerroue, E., Allen, P. A., Cozzi, A., Etienne, J. L. & Fanning, M. 50 million year duration negative carbon isotope excursion in the Ediacaran ocean. *Terra Nova* **18**, 147–153 (2006).
34. Bowring, S. A. *et al.* Geochronologic constraints on the chronostratigraphic framework of the Neoproterozoic Huqf Supergroup, sultanate of Oman. *Am. J. Sci.* **307**, 1097–1145 (2007).
35. Corsetti, F. A. & Kaufman, A. J. Stratigraphic investigations of carbon isotope anomalies and Neoproterozoic ice ages in Death Valley, California. *Geol. Soc. Am. Bull.* **115**, 916–932 (2003).
36. Kaufman, A. J., Corsetti, F. A. & Varni, M. A. The effect of rising atmospheric oxygen on carbon and sulfur isotope anomalies in the Neoproterozoic Johnnie Formation, Death Valley, USA. *Chem. Geol.* **237**, 47–63 (2007).
37. Verdel, C., Wernicke, B. P. & Bowring, S. A. The Shuram and subsequent Ediacaran carbon isotope excursions from southwest Laurentia, and implications for environmental stability during the metazoan radiation. *Geol. Soc. Am. Bull.* doi:10.1130/B30369.1 (in the press).
38. Condon, D. *et al.* U-Pb ages from the Neoproterozoic Doushantuo Formation, China. *Science* **308**, 95–98 (2005).
39. Jiang, G., Kaufman, A. J., Christie-Blick, N., Zhang, S. & Wu, H. Carbon isotope variability across the Ediacaran Yangtze platform in South China: implications for a large surface-to-deep ocean $\delta^{13}\text{C}$ gradient. *Earth Planet. Sci. Lett.* **261**, 303–320 (2007).
40. McFadden, K. A. *et al.* Pulsed oxidation and biological evolution in the Ediacaran Doushantuo Formation. *Proc. Natl Acad. Sci. USA* **105**, 3197–3202 (2008).
41. Calver, C. R. Isotope stratigraphy of the Ediacaran (Neoproterozoic III) of the Adelaide Rift Complex, Australia, and the overprint of water column stratification. *Precamb. Res.* **100**, 121–150 (2000).
42. Macdonald, F. A., Jones, D. S. & Schrag, D. P. Stratigraphic and tectonic implications of a newly discovered glacial diamictite-cap carbonate couplet in southwestern Mongolia. *Geology* **37**, 123–126 (2009).
43. Melezhik, V. A., Fallick, A. E. & Kuznetsov, A. B. Palaeoproterozoic, rift-related, ^{13}C -rich, lacustrine carbonates, NW Russia—Part II: Global isotope signal recorded in the lacustrine dolostones. *Earth Sci.* **95**, 423–444 (2005).
44. Prave, A. R., Fallick, A. E., Thomas, C. W. & Graham, C. M. A composite C-isotope profile for the Neoproterozoic Dalradian Supergroup of Scotland and Ireland. *J. Geol. Soc.* **166**, 845–857 (2009).
45. Canfield, D. E., Poulton, S. W. & Narbonne, G. M. Late-Neoproterozoic deep-ocean oxygenation and the rise of animal life. *Science* **315**, 92–95 (2007).
46. Sperling, E. A., Pisani, D. & Peterson, K. J. in *The Rise and Fall of the Ediacaran Biota* (eds Vickers-Rich, P. & Komarower, P.) 355–368 (The Geological Society Special Publications, 2007).
47. McCarron, M. E. G. *The Sedimentology and Chemostratigraphy of the Nafun Group, Huqf Supergroup, Oman* PhD thesis, Oxford Univ. (2000).
48. Knauth, L. P. & Kennedy, M. J. The late Precambrian greening of the Earth. *Nature* **460**, 728–732 (2009).
49. Derry, L. A. A burial diagenesis origin for the Ediacaran Shuram-Wonoka western isotope anomaly. *Earth Planet. Sci. Lett.* **294**, 152–162 (2010).
50. Hagadorn, J. W. & Waggoner, B. M. in *Abstracts with Programs, Annual Meeting Vol. 30*, 233 (Geological Society of America, 1998).
51. Kaufman, A. J., Jiang, G., Christie-Blick, N., Banerjee, D. & Rai, V. Stable isotope record of the terminal Neoproterozoic Krol platform in the Lesser Himalayas of northern India. *Precamb. Res.* **147**, 156–185 (2006).
52. Gaucher, C., Sial, A. N., Halverson, G. P. & Frimmel, H. E. in *Neoproterozoic-Cambrian Tectonics, Global Change And Evolution: A Focus On South West Gondwana* (eds Gaucher, C., Sial, A. N., Frimmel, H. E. & Halverson, G. P.) Ch. 1, 3–11 (Developments in Precambrian Geology Vol. 16, Elsevier, 2009).
53. Pokrovskii, B. G., Melezhik, V. A. & Bujakaite, M. I. Carbon, oxygen, strontium, and sulfur isotopic compositions in Late Precambrian rocks of the Patom Complex, central Siberia: Communication 1. results, isotope stratigraphy, and dating problems. *Lithol. Miner. Resour.* **41**, 450–474 (2006).
54. Summa, C. L. *Sedimentologic, Stratigraphic, and Tectonic Controls of a Mixed Carbonate-Siliciclastic Succession: Neoproterozoic Johnnie Formation, Southeast California* (Massachusetts Institute of Technology, 1993).
55. Haines, P. W. in *The Evolution of a Late Precambrian-Early Palaeozoic Rift Complex, Adelaide Geosyncline* (eds Jago, J. B. & Moore, P. S.) 177–198 (Geological Society of America Special Publication 16, 1990).
56. Kump, L. R. Interpreting carbon-isotope excursions, Strangelove oceans. *Geology* **19**, 299–302 (1991).
57. Derry, L. A. On the significance of $\delta^{13}\text{C}$ correlations in ancient sediments. *Earth Planet. Sci. Lett.* **296**, 497–501 (2010).
58. Dehler, C. M. *et al.* High-resolution $\delta^{13}\text{C}$ stratigraphy of the Chuar Group (ca. 770–742 Ma), Grand Canyon: Implications for mid-Neoproterozoic climate change. *GSA Bull.* **117**, 32–45 (2005).
59. Bristow, T. F. & Kennedy, M. J. Carbon isotope excursions and the oxidant budget of the Ediacaran atmosphere and ocean. *Geology* **36**, 863–866 (2008).
60. Bjerrum, C. J. & Canfield, D. E. Towards a quantitative understanding of the late Neoproterozoic carbon cycle. *Proc. Natl Acad. Sci. USA* doi:10.1073/pnas.1101755108 (2011).
61. Brand, U. & Veizer, J. Chemical diagenesis of a multicomponent carbonate system-1: Trace elements. *J. Sedim. Petrol.* **50**, 1219–1236 (1980).
62. Grover, G. Jr. & Read, J. F. Paleoquifer and deep burial related cements defined by regional cathodoluminescent patterns, Middle Ordovician carbonates, Virginia. *AAPG Bull.* **67**, 1275–1303 (1983).
63. Meyers, W. J. & Lohmann, K. C. in *Carbonate Cements* Vol. 36 (eds Schneiderman, N. & Harris, P. M.) 223–240 (Society of Economic Paleontologists and Mineralogists Special Publication, 1985).
64. Zempolich, W. G., Wilkinson, B. H. & Lohmann, K. C. Diagenesis of late Proterozoic carbonates: the Beck Spring Dolomite of eastern California. *J. Sedim. Petrol.* **58**, 656–672 (1988).
65. Derry, L. A., Kaufman, A. J. & Jacobsen, S. B. Sedimentary cycling and environmental change in the Late Proterozoic: evidence from stable and radiogenic isotopes. *Geochim. Cosmochim. Acta* **56**, 1317–1329 (1992).
66. Kaufman, P., Grotzinger, J. P. & McCormick, D. S. in *Sedimentary Modeling: Computer Simulations and Methods for Improved Parameter Definition* Vol. 233 (eds Franseen, E. K., Watney, W. L., Kendall, C. G. St. C. & Ross, W.) 489–508 (Kansas Geological Survey, 1991).
67. Asmeron, Y., Jacobsen, S. B., Knoll, A. H., Butterfield, N. J. & Swett, K. Strontium isotopic variations of Neoproterozoic seawater: implications for crustal evolution. *Geochim. Cosmochim. Acta* **55**, 2883–2894 (1991).
68. Vogel, J. C. in *Stable Isotopes and Plant Carbon-Water Relations* (eds Ehleringer, J. R., Hall, A. E. & Farquhar, G. D.) 29–38 (Academic, 1993).
69. Swart, P. K. & Eberli, G. E. The nature of the $\delta^{13}\text{C}$ of periplatform sediments: implications for stratigraphy and the global carbon cycle. *Sedim. Geol.* **175**, 115–129 (2005).

70. Melim, L. A., Swart, P. K. & Malivia, R. G. in *Subsurface Geology of Prograding Carbonate Platform Margin, Great Bahamas Bank* Vol. 70 (ed. Ginsburg, R. N.) 137–161 (SEPM Special Publication, 2001).
71. Gray, J., Chaloner, W. & Westoll, T. The microfossil record of early land plants: advances in understanding of early terrestrialization. *Biol. Sci.* **309**, 167–195 (1985).
72. Steemans, P. & Wellman, C. H. in *The Great Ordovician Biodiversification Event* (eds Webby, B. *et al.*) 361–366 (Columbia Univ. Press, 2004).
73. Gensel, P. G. The earliest land plants. *Annu. Rev. Ecol. Evol. Syst.* **39**, 459–477 (2008).
74. Arthur, M. A. Paleocceanographic events - recognition, resolution, and reconsideration. *Rev. Geophys. Space Phys.* **17**, 1474–1494 (1979).
75. Moore, C. H. & Druckman, Y. D. Burial diagenesis and porosity evolution, Upper Jurassic Smackover, Arkansas and Louisiana. *AAPG Bull.* **65**, 597–628 (1981).
76. Visser, W. Burial and thermal history of Proterozoic source rocks in Oman. *Precamb. Res.* **54**, 15–36 (1991).
77. Terken, J. M. J. & Freewin, N. L. The Dhahaban petroleum system of Oman. *AAPG Bull.* **84**, 523–544 (2000).
78. Terken, J. M. J., Frewin, N. L. & Indrelid, S. L. Petroleum systems of Oman: charge timing and risks. *AAPG Bull.* **85**, 1817–1845 (2001).
79. Moldovanyi, E. P. & Walter, L. M. Regional trends in water chemistry, Smackover Fm., southwest Arkansas: geochemical and physical contents. *AAPG Bull.* **76**, 864–894 (1992).
80. Heydari, H. & Moore, C. Burial diagenesis and thermochemical sulfate reduction, Smackover Formation, southeastern Mississippi salt basin. *Geology* **17**, 1080–1084 (1989).
81. Pelechaty, S. M., Grotzinger, J. P., Kashirtsev, V. A. & Jerinovsky, V. P. Chemostratigraphic and sequence stratigraphic constraints on Vendian-Cambrian basin dynamics, northeast Siberian craton. *J. Geol.* **104**, 543–564 (1996).
82. Knoll, A. H., Grotzinger, J. P., Kaufman, A. J. & Kolosov, P. Integrated approaches to terminal Proterozoic stratigraphy: an example from the Olenek uplift, northeastern Siberia. *Precamb. Res.* **73**, 251–270 (1995).
83. Pelechaty, S. M., Kaufman, A. J. & Grotzinger, J. P. Evaluation of $d^{13}C$ isotope stratigraphy for intrabasinal correlation: Vendian strata of the Olenek uplift and Kharaulakh Mountains, Siberian platform, Russia. *Geol. Soc. Am. Bull.* **108**, 992–1003 (1996).
84. Swanson-Hysell, N. L. *et al.* Cryogenian glaciation and the onset of carbon-isotope decoupling. *Science* **328**, 608–611 (2010).
85. Krijgsman, W., Hilgen, F. J., Raffi, I., Sierro, F. J. & Wilson, D. S. Chronology, causes and progression of the Messinian salinity crisis. *Nature* **400**, 652–655 (1999).
86. Alvarez, W. & Assaro, F. An extraterrestrial impact. *Sci. Am.* **263**, 78–84 (1990).
87. Courtillot, V. *Evolutionary Catastrophes: The Science of Mass Extinction* (Cambridge Univ. Press, 1999).
88. Bowring, S. A. *et al.* U/Pb zircon geochronology and tempo of the end-Permian mass extinction. *Science* **280**, 1039–1045 (1998).
89. Mundil, R., Ludwig, K. R., Metcalfe, I. & Renne, P. Age and timing of the Permian mass extinctions: U/Pb dating of closed-system zircons. *Science* **305**, 1760–1763 (2004).
90. Hoffman, P. F. & Schrag, D. P. The Snowball Earth hypothesis: testing the limits of global change. *Terra Nova* **14**, 129–155 (2002).
91. Banner, J. & Kaufman, J. The isotopic record of ocean chemistry and diagenesis preserved in non-luminescent brachiopods from Mississippian carbonate rocks, Illinois and Missouri. *Bull. Geol. Soc. Am.* **106**, 1074–1082 (1994).
92. Braithwaite, C. & Montaggioni, L. The Great Barrier Reef: a 700,000 year diagenetic history. *Sedimentology* **56**, 1591–1622 (2009).
93. Pelechaty, S. M., James, N. P., Kerans, C. & Grotzinger, J. P. A middle Proterozoic paleokarst unconformity and associated rocks, Elu Basin, northwest Canada. *Sedimentology* **38**, 775–797 (1991).
94. Kenny, R. & Knauth, L. P. Stable isotope variations in the Neoproterozoic Beck Spring Dolomite and Mesoproterozoic Mescal Limestone paleokarst: implications for life on land in the Precambrian. *GSA Bull.* **113**, 650–658 (2001).
95. Pisarevsky, S. A., Murphy, J. B., Cawood, P. A. & Collins, A. S. Late Neoproterozoic and Early Cambrian palaeogeography: models and problems 9–31 (The Geological Society Special Publications 294, 2008).

Acknowledgements

We thank the Agouon Institute and the NASA Astrobiology Institute for support. T. Raub helped with construction of Fig. 2. K. Bergmann supplied the image in Fig. 4b. M. Saltzman is acknowledged for sharing pre-publication composite carbon isotope data used to construct Fig. 1, and C. Verdel and B. Wernicke are thanked for sharing pre-publication data for the Johnnie Formation shown in Fig. 3. L.

Author contributions

J.G., D.F. and W.F. each contributed by writing the text, drafting the figures and participating in data analysis. These responsibilities were divided equally.

Additional information

The authors declare no competing financial interests.